

This is a repository copy of *Fetal glycosylation defect due to ALG3 and GOG5 variants detected via amniocentesis : complex glycosylation defect with embryonic lethal phenotype*.

White Rose Research Online URL for this paper:

<https://eprints.whiterose.ac.uk/168123/>

Version: Accepted Version

---

## Article:

Ferrer, Alejandro, Tzovenos Starosta, Rodrigo, Ranatunga, Wasantha et al. (6 more authors) (2020) Fetal glycosylation defect due to ALG3 and GOG5 variants detected via amniocentesis : complex glycosylation defect with embryonic lethal phenotype. *Molecular genetics and metabolism*. pp. 424-429. ISSN 1096-7192

<https://doi.org/10.1016/j.ymgme.2020.11.003>

---

## Reuse

This article is distributed under the terms of the Creative Commons Attribution-NonCommercial-NoDerivs (CC BY-NC-ND) licence. This licence only allows you to download this work and share it with others as long as you credit the authors, but you can't change the article in any way or use it commercially. More information and the full terms of the licence here: <https://creativecommons.org/licenses/>

## Takedown

If you consider content in White Rose Research Online to be in breach of UK law, please notify us by emailing [eprints@whiterose.ac.uk](mailto:eprints@whiterose.ac.uk) including the URL of the record and the reason for the withdrawal request.

1 Fetal glycosylation defect due to *ALG3* and *GOG5* variants detected via  
2 amniocentesis: complex glycosylation defect with embryonic lethal phenotype

3 Alejandro Ferrer<sup>1,\*</sup> Rodrigo Tzovenos Starosta<sup>2,3,\*</sup> Wasantha Ranatunga<sup>2</sup>, Dani Ungar<sup>4</sup>, Tamas  
4 Kozicz<sup>1</sup>, Eric Klee<sup>1</sup>, Laura M. Rust<sup>2,5</sup>, Myra Wick<sup>2,5</sup>, Eva Morava<sup>1,2,6\*\*</sup>

5 1 – Center for Individualized Medicine, Mayo Clinic, Rochester, MN, USA

6 2 – Department of Clinical Genomics, Mayo Clinic, Rochester, MN, USA

7 3 – Graduate Program in Genetics and Molecular Biology, Universidade Federal do Rio Grande  
8 do Sul, Porto Alegre, RS, Brazil

9 4 – Department of Biology, University of York, York, UK

10 5 – Department of Obstetrics and Gynecology, Mayo Clinic, Rochester, MN, USA

11 6 – Department of Laboratory Medicine and Pathology, Mayo Clinic, Rochester, MN, USA

12

13 \*Contributed equally to the manuscript

14

15 \*\*Corresponding author:

16 Eva Morava

17 Mayo Clinic

18 200 1<sup>st</sup> St SW

19 Rochester, MN 55905, USA

20 Email: morava-kozicz.eva@mayo.edu

21

22 AF, TK and EM designed the study. EM obtained funding. LMR and EM conducted the  
23 consenting process. AF, RTS, EK, LMR, MJW, and EM reviewed the case. RTS, DU and TK  
24 designed the experiments. RTS and WR conducted all experiments. AF and EK performed the  
25 bioinformatic analysis. AF and RTS wrote the original draft. WR, DU, TK, EK, LMR, MJW and  
26 EM reviewed the draft and made important intellectual contributions. EM obtained funding and  
27 coordinated the study. EM made the final decision to submit the manuscript and is the guarantor  
28 to this work.

29

30 Keywords: congenital disorders of glycosylation; osteochondrodysplasia; fetal cell research; fetal  
31 demise; whole-exome sequencing

32 ABSTRACT

33 **Introduction:** Congenital disorders of glycosylation (CDG) are inborn errors of glycan  
34 metabolism with high clinical variability. Only a few antenatal cases have been described with  
35 CDG. Due to a lack of reliable biomarker, prenatal CDG diagnostics relies primarily on  
36 molecular studies. In the presence of variants of uncertain significance prenatal glycosylation  
37 studies are very challenging.

38 **Case Report:** A consanguineous couple had a history of second-trimester fetal demise with  
39 tetralogy of Fallot and skeletal dysplasia. In the consecutive pregnancy, the second trimester  
40 ultrasonography showed skeletal dysplasia, vermian hypoplasia, congenital heart defects,  
41 omphalocele and dysmorphic features. Prenatal chromosomal microarray revealed a large region  
42 of loss of heterozygosity. Demise occurred at 30 weeks. Fetal whole exome sequencing showed a  
43 novel homozygous likely pathogenic variant in *ALG3* and a variant of uncertain significance in  
44 *COG5*.

45 **Methods:** Western blot was used to quantify *ALG3*, *COG5*, *COG6*, and the glycosylation  
46 markers ICAM-1 and LAMP2. RT-qPCR was used for *ALG3* and *COG5* expression in cultured  
47 amniocytes and compared to age matched controls.

48 **Results:** *ALG3* and *COG5* mRNA levels were normal. ICAM-1, LAMP2, *ALG3* and *COG5*  
49 levels were decreased in cultured amniocytes, suggesting the possible involvement of both genes  
50 in the complex phenotype.

51 **Conclusion:** This is the first case of successful use of glycosylated biomarkers in amniocytes,  
52 providing further options of functional antenatal testing in CDG.

53 INTRODUCTION

54 Congenital disorders of glycosylation (CDG) are a growing group of rare inherited metabolic  
55 disorders that affect the building and processing of glycans. The clinical manifestations of CDG  
56 vary depending on the biochemical defect (the impacted glycosylation step) and the molecular  
57 background. Due to the extreme rarity of these disorders, for many CDG the full clinical  
58 spectrum is not yet known; many of those disorders have a complex, multisystem phenotype  
59 including malformations, early-onset metabolic abnormalities, and organ dysfunction. CDG are  
60 classified primarily according to the type of glycosylation affected – N-glycosylation  
61 (attachment of glycans to the amide group of asparagine residues in proteins) or O-glycosylation  
62 (attachment of glycans to the lateral oxygen atom of serine or threonine residues). CDG affecting  
63 N-glycosylation are further divided according to whether they affect the assembly of glycans in  
64 the endoplasmic reticulum (CDG-I) or the remodeling of those glycans either in the endoplasmic  
65 reticulum or the Golgi apparatus (CDG-II). With the implementation of next-generation  
66 sequencing (NGS) in clinical practice, the knowledge of the genetic etiology of CDG has  
67 expanded enormously with more than 137 different CDG discovered to date (1).

68 We report a consanguineous couple with two spontaneous pregnancy losses in which the  
69 fetuses presented with a similar abnormal phenotype. Whole exome sequencing (WES) of  
70 amniocyte DNA obtained from the second miscarriage identified a homozygous missense variant  
71 in *COG5* and a homozygous nonsense variant in *ALG3* that were also confirmed by PCR in the  
72 first miscarriage. These two genes are included in the N-glycosylation pathway and potentially  
73 contributory to fetal demise (2-4). However, both variants were novel and therefore further  
74 research testing was pursued.

75

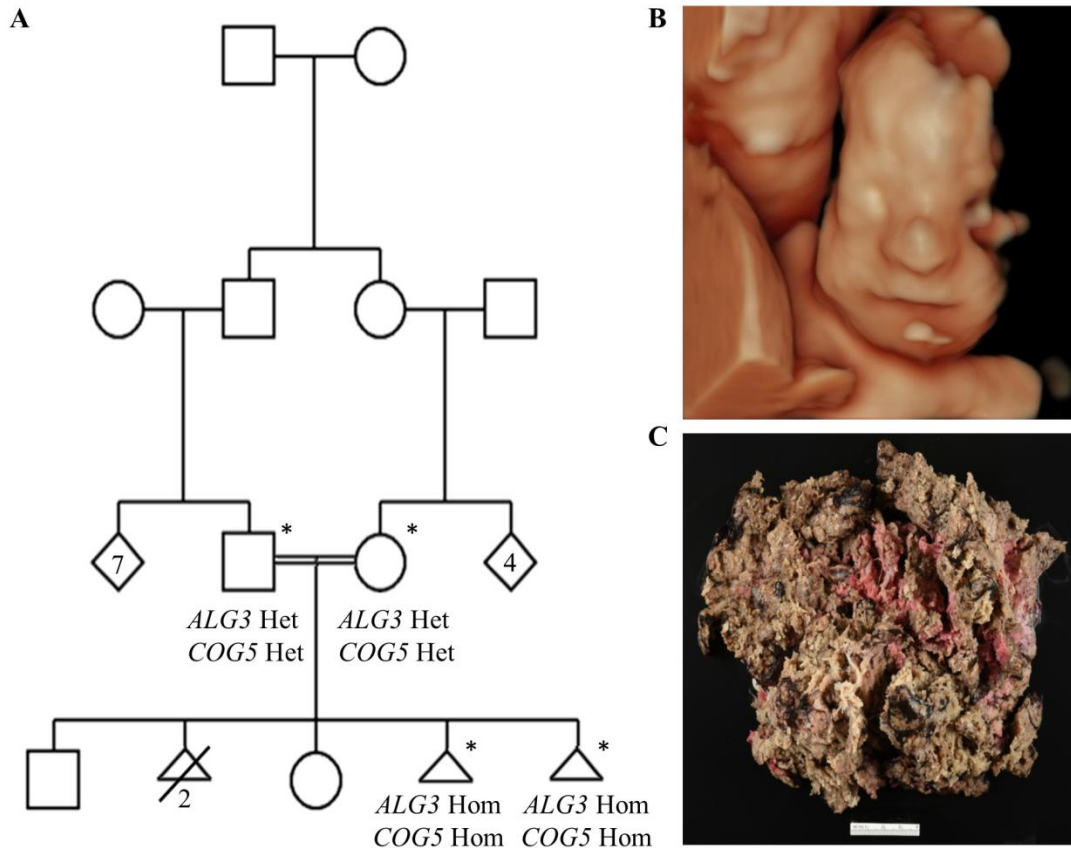
## 76 CASE REPORT

77 A 28-year-old G6P2122 woman at 12 3/7 weeks gestational age presented for genetic  
78 counseling due to a history of previous fetal demise, family history of spinal muscular atrophy,  
79 and consanguinity (figure 1A). She and her partner, both of Pakistani ancestry, are the parents of  
80 two healthy children, aged 8 and 5 years. The couple also had a pregnancy which resulted in  
81 intrauterine fetal demise at 24 4/7 weeks; autopsy revealed tetralogy of Fallot, probable skeletal  
82 dysplasia with decreased long bone length (<2<sup>nd</sup> percentile for gestational age), and dysmorphic  
83 findings including micrognathia, slit-like nostrils, and flat upper lip. Chromosomal microarray  
84 (CMA) was negative for deletions or duplications, but revealed large regions with loss of  
85 heterozygosity (LOH) presumably due to consanguinity (approximately 8%). The patient's  
86 obstetrical history also included two first trimester elective terminations.

87 At 17 weeks gestation of the current pregnancy, early anatomical ultrasound revealed similar  
88 anomalies to the prior affected pregnancy (figure 1B) including skeletal dysplasia with  
89 shortening of all long bones, short ribs, micrognathia, small nose, vermian hypoplasia, and  
90 congenital heart defect. The fetus had the additional finding of an omphalocele and echogenic  
91 bowel. Amniocentesis was performed and CMA was negative for deletions and duplications, but  
92 revealed 15% LOH.

93 At 30-1/7 weeks gestational age, the patient experienced preterm onset of labor resulting in  
94 delivery of a stillborn infant. The placenta was large-for-gestational-age, friable, and hydropic on  
95 pathological examination (figure 1C). WES performed on amniocytes from this second  
96 pregnancy identified two homozygous variants of interest (*COG5* c.944C>G, p.Ser315Cys; and  
97 *ALG3* c.1188G>A, p.Trp396\*) inherited from both healthy, heterozygous carriers parents.

98 Consequently, placental tissue from the first pregnancy was tested by directed PCR and found to  
99 also carry both variants.



100

101 Figure 1: A) Pedigree of the family showing a high degree of consanguinity. Asterisks indicate  
102 individuals genetically tested. The genotypes for the variants in *ALG3* and *COG5* are indicated  
103 under each symbol. Het: heterozygous, Hom: homozygous. B) Tridimensional reconstruction of  
104 fetal ultrasound at gestational age 24 weeks, 6 days showing hypertelorism, depressed nasal  
105 bridge, and thin upper lip of the fetus. C) Photograph of the fetal surface of the placenta, showing  
106 hydropic, partially disintegrated villi.

107

## 108 METHODS

### 109 **Whole Exome Sequencing Analysis**

110 WES from the second miscarriage and both parents was performed at the Clinical Genomics  
111 Laboratory (Mayo Clinic). Paired-end libraries were prepared using 1.0 µg of genomic DNA  
112 using the Agilent Bravo liquid handler (Agilent) as indicated by the manufacturer. Whole exon  
113 capture was carried out using 750 ng of the prepped library following the protocol for Agilent's  
114 SureSelect Human All Exon v5 + UTRs 75 MB kit. The purified capture products were  
115 amplified using the SureSelect Post-Capture Indexing forward and Index PCR reverse primers  
116 (Agilent) for 12 cycles. Libraries were sequenced at an average coverage of ~80X following  
117 Illumina's standard protocol in an Illumina cBot and HiSeq 3000/4000 PE Cluster Kit. The flow  
118 cells were sequenced as 150 X 2 paired end reads on an Illumina HiSeq 4000 using HiSeq  
119 3000/4000 sequencing kit and HCS v3.3.52 collection software. Base-calling is performed using  
120 Illumina's RTA version 2.7.3. Data was processed through an in-house bioinformatics pipeline  
121 and analyzed using Ingenuity (Qiagen) by the Center for Individualized Medicine (Mayo Clinic).

### 122 **Variant Segregation Testing**

123 A formalin-fixed, paraffin embedded (FFTE) sample from the placenta of the first  
124 miscarriage was used for testing and was used to obtain genomic DNA following a standard  
125 clinical procedure. The presence of both the homozygous *COG5* and *ALG3* variants found in the  
126 second miscarriage was tested by PCR using the primers described in Table 1 and the Platinum  
127 TaqDNA polymerase High Fidelity commercial kit (ThermoFisher Scientist) following the  
128 manufacturer indications. The conditions for the melting step were 51°C (for *COG5*) or 53°C (for  
129 *ALG3*) for 30 s.

130 **Table 1.** Primers used for targeted sequencing of *COG5* and *ALG3* variants and mRNA  
 131 expression levels by RT-PCR .

Gene Symbol	Test	Oligonucleotide Sequence	Orientation	Predicted Size
<i>COG5</i>	Family segregation of c.944C>G variant	5'-CTCAATAAATTATTTCTAAAGAAGGA-3'	Forward	465 bp
		5'-CAATACTTTTTGTAGATGTTGTACCT-3'	Reverse	
<i>ALG3</i>	Family segregation of c.1188G>A variant	5'-CATACAGATCGTTTCTACCCTCT-3'	Forward	446 bp
		5'-GTGGGCTTCTTGCTGT-3'	Reverse	
<i>COG5</i>	mRNA expression	5'- TGGGTCCATTCTGTAGACGA-3'	Forward	N/A
		5'- GTTCACTTGCCTGGAAGAGC-3'	Reverse	
<i>ALG3</i>	mRNA expression	5'-CACCTTCTGGGTCATTCACAGG-3'	Forward	N/A
		5'- GTGTCACCCTGCAGTTGGGTATAGT-3'	Reverse	
<i>RNA18S</i>	mRNA expression	5'-GTAACCCGTTGAACCCCAT-3'	Forward	N/A
		5'-CCATCCAATCGGTAGTAGCG-3'	Reverse	
<i>GAPDH</i>	mRNA expression	5'-GCCAAAAGGGTCATCATCTC-3'	Forward	N/A
		5'-GGCCATCCACAGTCTTCT-3'	Reverse	
<i>ACTB</i>	mRNA expression	5'-CATGTACGTTGCTATCCAGGC-3'	Forward	N/A
		5'-CTCCTTAATGTCACGCACGAT-3'	Reverse	

132

### 133 Amniocyte Culture

134 Amniocytes were obtained from the amniocentesis during the second pregnancy. Primary  
 135 cultures were established for 9 days before transferring to T25 culture flasks. Cells were  
 136 incubated at 37°C with 5% CO<sub>2</sub>, 5% O<sub>2</sub> and 90% N<sub>2</sub> in 50% Chang C Working Medium (Irvine)  
 137 and 50% Dulbecco's Modified Eagle Medium Alpha with GlutaMAX (Gibco) supplemented  
 138 with 12.5% fetal bovine serum (Gibco) and 1% Penicillin/Streptomycin solution (Gibco).

### 139 Western blot

140 Protein extracts from amniocytes were denatured for either 30 minutes at 70°C (ICAM-1 and  
 141 LAMP2) or 5 minutes at 95°C (ALG3, COG5 and COG6) in dithiothreitol (DTT) or β-  
 142 mercaptoethanol and LDS-containing NuPAGE sample buffer (Novex and Invitrogen, Carlsbad,  
 143 CA, USA) and loaded into either a 10% (ICAM-1 and ALG3) or a 4-12% (LAMP2, COG5, and  
 144 COG6) Bis-Tris gel (Invitrogen). Electrophoresis was performed in MOPS SDS NuPAGE



145 running buffer (Novex) at 200V for 60 minutes, followed by transfer to a nitrocellulose  
146 membrane (Bio-Rad laboratories, Germany) in NuPAGE transfer buffer (Novex) at 35V for 180  
147 minutes. Membranes were blocked at either SEA Block blocking buffer (Thermo Scientific,  
148 Rockford, IL, USA) (ICAM-1) or 5% blocking-grade non-fat milk (Sigma Aldrich, Saint Louis,  
149 MO, USA) or 5% BSA in Tris buffered saline with 0.1% Tween-20 (TBST). Primary antibodies  
150 (ICAM-1 mouse monoclonal, Santa Cruz Biotechnology, 1:500; LAMP2 mouse monoclonal,  
151 H4B4 clone, Invitrogen, 1:1000; ACTB rabbit monoclonal antibody, ABclonal, 1:10,000;  
152 GAPDH mouse monoclonal antibody, Invitrogen, 1:20,000; ALG3 rabbit polyclonal, 1:125,  
153 Abnova; COG5 rabbit polyclonal and COG6 rabbit polyclonal provided in house (5), University  
154 of York, UK, 1:500) were incubated overnight or 48-72 hours at 4°C and washed with 0.1%  
155 Tween-20 in PBS or TBST (Fisher Bioreagents, Fair Lawn, NJ, USA). For ICAM-1, LAMP2,  
156 ALG3, ACTB and GAPDH, a fluorescent-conjugated secondary antibody (donkey anti-mouse  
157 cross-adsorbed secondary antibody, DyLight 800 conjugate; donkey anti-rabbit cross-adsorbed  
158 secondary antibody, DyLight 680 conjugate; both from Invitrogen) was used. For COG5 and  
159 COG6, a biotinylated secondary antibody (Biotin-SP-conjugated AffiniPure donkey anti-rabbit,  
160 Jackson ImmunoResearch Laboratories, West Grove, PA, USA, 1:1000) was used. Secondary  
161 antibodies were incubated for 1 hour at 4°C, washed with 0.1% Tween-20 in PBS, and  
162 membranes were either detected and quantified in an Odyssey Fc system (Li-Cor Biosciences,  
163 Lincoln, NE, USA) or incubated in fluorophore-conjugated streptavidin (AlexaFluor 680-  
164 conjugated streptavidin, Jackson ImmunoResearch Laboratories, 1:1000) for 30 min at 4°C.  
165 After incubation with streptavidin, membranes were washed with 0.1% Tween-20 in PBS,  
166 detected and quantified in the same Odyssey Fc system.

#### 167 **Real-time quantitative polymerase chain reaction (RT-qPCR)**

168 Isolated RNA from amniocytes was reversed transcribed to cDNA using the SuperScript III  
169 First-Strand kit (Invitrogen) according to the manufacturer's protocol (primer sequences were  
170 synthesized by Integrated DNA Technologies, Coralville, IA, USA and are available in Table 1).  
171 The reverse-transcriptase polymerase chain reaction (RT-PCR) was set up using the following  
172 conditions: 65°C for 5 minutes, 25°C for 10 minutes, 50°C for 50 minutes, 85°C for 5 minutes.  
173 For the real-time quantitative polymerase chain reaction (RT-qPCR) mixtures contained each  
174 6.05 µL SYBR Green (Applied Biosystems, Warrington, UK), 3.63 µL double deionized H<sub>2</sub>O,  
175 1.21 µL of the respective primers, and 1.1 µL of cDNA. RT-qPCR cycles were performed and  
176 read in a LightCycler 480 II (Roche Molecular Systems, Rotkreuz, Switzerland) as follows: pre-  
177 incubation at 95°C for 5 minutes; 45 cycles of amplification at 95°C for 10 seconds, 60°C for 10  
178 seconds, 72°C for 10 seconds; melting curve at 95°C for 5 seconds and 65°C for 1 minute; and  
179 cooling at 40°C for 30 seconds.

## 180 RESULTS

### 181 Genetic Analysis

182 The analysis of WES data focused on the overlapping LOH areas observed by CMA in both  
183 miscarriages, where only three genes (*EDEM3*, *TMEM140* and *COG5*) were found to carry  
184 homozygous rare (below 1% in healthy population (6)) variants. An in-depth review of these  
185 results concluded that the variant in *COG5* (c.944C>G; p.Ser315Cys) potentially explained the  
186 patient's phenotype. Interestingly, further review identified an additional gene in *N*-glycosylation  
187 pathway (*ALG3* – c.1188G>A; p.Trp396\*) carrying a homozygous likely pathogenic variant.

188 The homozygous c.944C>G; p.Ser315Cys variant in *COG5* is a novel variant not reported in  
189 the healthy population (gnomAD (6)) or variants databases (ClinVar and HGMD). The amino

190 acid position is not conserved across species and it is not located in any functional domain  
191 described. Some *in silico* predictions suggested a deleterious effect (SIFT, PolyPhen,  
192 MutationTaster) although in other cases (M-CAP) was predicted as benign. The constraint values  
193 described in gnomAD for this gene indicate tolerance to missense variation. We classified the  
194 variant as uncertain significance (VUS) according to ACMG criteria but it was considered  
195 relevant due to the possible phenotypic overlap between the two fetuses and other CDG patients  
196 including skeletal dysplasia.

197 On the other hand, the homozygous c.1188G>A; p.Trp396\* variant in *ALG3* is classified as  
198 likely pathogenic by ACMG criteria but the possible connection with the phenotype observed  
199 was not clear. This variant was not present in the healthy population (gnomAD (6)) or variant  
200 databases (ClinVar and HGMD). The variant is located in the last exon of the protein and does  
201 not impact any functional domain described. It is not predicted to initiate nonsense mediated  
202 decay by the 50bp rule but the constraint values described in gnomAD for this gene indicate  
203 intolerance to loss of function variations.

204 Both variants were also detected in the first miscarriage after testing the genomic DNA  
205 obtained from a formalin-fixed, paraffin embedded (FFTE) sample by PCR. Unfortunately,  
206 healthy siblings were not available for testing.

## 207 **Glycosylation markers**

208 N-glycosylation markers ICAM1 and LAMP2 analyzed by Western blot were both abnormal  
209 in cultured amniocytes from the affected individual compared to cultured amniocyte controls,  
210 confirming a glycosylation defect. Decreased abundance of glycosylated ICAM-1 was detected  
211 in cultured amniocytes (the protein expression was 61.4% lower than that in control amniocytes),

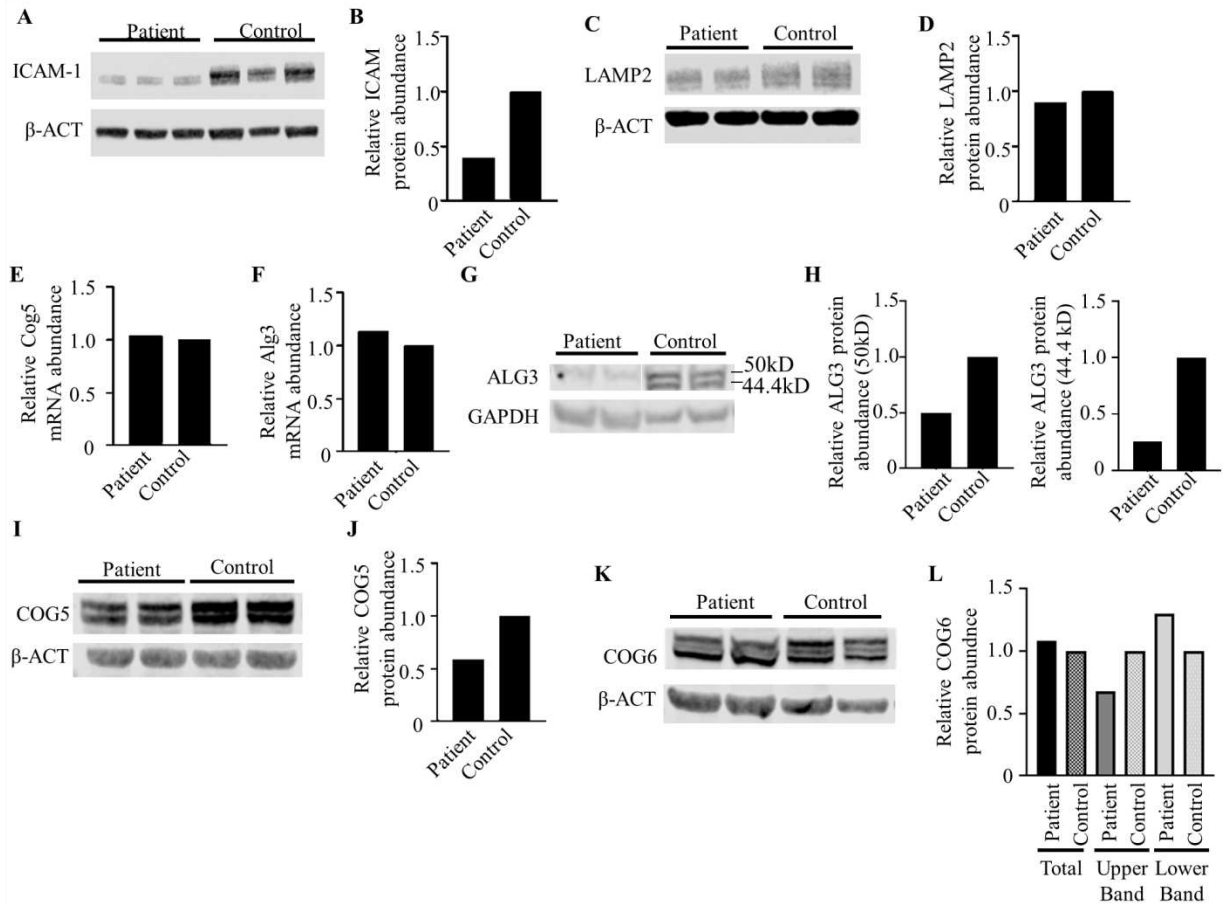
212 as shown in figure 2A and B. The LAMP2 protein showed an abnormal migration pattern by  
213 Western blot, compatible with abnormal LAMP2 glycosylation in the affected individuals  
214 amniocytes compared to controls (figure 2C and D).

### 215 **Gene expression of *ALG3* and *COG5***

216 Gene expression studies by RT-qPCR showed no decrease in the level of gene products for  
217 either *ALG3* or *COG5* genes, additionally excluding nonsense-mediated decay in the case of  
218 *ALG3*. Levels of *Cog5* mRNA were similar between affected individual and control amniocytes  
219 (figure 2E) while *Alg3* mRNA levels were slightly higher in the affected individual's amniocytes  
220 (figure 2F).

### 221 **Protein expression of *ALG3*, *COG5* and *COG6***

222 Protein expression of *ALG3*, *COG5* and *COG6* (another subunit from the same COG lobe)  
223 were all decreased in the affected individual's amniocytes compared to the control amniocytes.  
224 The *ALG3* Western blot showed two bands corresponding to the two different isoforms of the  
225 protein (50kD and 44kD) that were both decreased by 49.8% and 74.3% respectively (Figure 2 G  
226 and H). Quantitation of *COG5* protein was found 41% lower compared to the control by Western  
227 blot, as shown in figure 2J. Similarly, Western blot analysis of *COG6* showed a double band  
228 (figure 2K and L): the upper band, which is appropriate for the predicted size of 68 kDa for  
229 *COG6*, was 34% decreased in the affected individual's amniocytes compared to controls. The  
230 lower band was 30% increased in the affected individual's amniocytes compared to controls  
231 (figure 2L). We hypothesize that this band may be the product of proteolytic degradation of  
232 *COG6*.



233

234 Figure 2: A) Representative Western blot of patient and control amniocytes against ICAM-1. B)   
 235 Quantification of Western blot shown in A indicating protein abundance 61.4% lower in the   
 236 patient, consistent with a glycosylation defect. C) Representative Western blot of patient and   
 237 control amniocytes against LAMP2. D) Quantification of Western blot shown in C indicating   
 238 protein abundance 11.4% lower in the patient, as well as an altered protein migration pattern in   
 239 the patient compared to control, consistent with a glycosylation defect. E) RT-qPCR of Cog5 in   
 240 patient amniocytes and control amniocytes, averaged against the three housekeeping transcripts   
 241 Rna18s, Gapdh, and Bact, showing approximately same levels of Cog5 mRNA. F) RT-qPCR of   
 242 Alg3 in patient amniocytes and control amniocytes, averaged against the three housekeeping   
 243 transcripts Rna18s, Gapdh, and Bact, showing an increase of 13.3% in mRNA abundance in the

244 patient. G) Representative Western blot of ALG3 expression in patient amniocytes and control  
245 amniocytes. Two bands are present (50kD and 44.4 kD) corresponding to each isoform of ALG3.  
246 H) Quantification of Western blot shown in G indicating a protein abundance 49.8% (50kD  
247 band) and 74.3% (44.4 kD) lower in the patient compared to control amniocytes. I)  
248 Representative Western blot against COG5 in patient amniocytes and control amniocytes. J)  
249 Quantification of Western blot shown in I indicating a protein abundance 41% lower in the  
250 patient compared to control amniocytes. K) Representative Western blot performed in patient  
251 and control amniocytes against COG6. L) Quantification of I showing a lower intensity of the  
252 upper band and a higher intensity of the lower band compared to control amniocytes.  $\beta$ -ACT:  $\beta$ -  
253 actin; GAPDH: Glyceraldehyde 3-phosphate dehydrogenase.

254

## 255 DISCUSSION

256 CDG are rare metabolic disorders that affect the assembly and processing of glycans, mainly  
257 in the endoplasmic reticulum (ER) and in the Golgi apparatus (7). The CDG group is extremely  
258 heterogeneous, ranging from diseases that are tissue-restricted (8) to multi-system organ  
259 involvement (9). In most rare CDG our current knowledge of the phenotypic spectrum is biased  
260 because it often relies on reports of a single or a few cases. CDG with early fetal loss thus tend to  
261 be underdiagnosed and underreported. For example, COG5-CDG, first described as a mild  
262 psychomotor delay syndrome (10), was reported in subsequent reports in patients with prenatal  
263 features who develop significant complications in multiple systems (11). This high variability  
264 also complicates the identification of the genetic cause resulting in the different manifestations of  
265 the disease.

266 Here we report on a consanguineous family with two spontaneous fetal demises showing  
267 similar timeframes and phenotype including a heart defect and signs of skeletal dysplasia. WES  
268 testing revealed two variants in genes included in the glycosylation pathway (homozygous VUS  
269 in *COG5* and homozygous likely pathogenic variants in *ALG3*) inherited from both parents who  
270 were both heterozygous carriers. Since both variants were confirmed by PCR to be also present  
271 in homozygosis in the first miscarriage, we hypothesized that the phenotype was caused by a  
272 glycosylation defect. We evaluated the N-glycosylation pathway in cultured amniocytes obtained  
273 from the second pregnancy by measuring two common glycosylation markers using Western  
274 blot: ICAM-1 and LAMP2. The expression of both proteins was abnormal compared to control  
275 amniocytes (Figure 2A-C). This combined deficit is expected in most CDG, even though  
276 decreased abundance of LAMP2 or ICAM-1 in isolation do not always reflect major expression  
277 changes in all CDG (12, 13). We performed RT-qPCR studies of gene expression of *COG5* and  
278 *ALG3* that indicated normal mRNA levels (Figure 2E and F), suggesting that the presence of the  
279 variants did not affect gene expression and a possible alteration would be at the protein level.

280 The protein levels of *ALG3* and *COG5* in the affected individual's sample by Western blot  
281 were markedly reduced compared to controls (Figure 2G to J). The reduction of *ALG3* protein  
282 levels could be explained by a higher degradation of the truncated protein as a consequence of  
283 the variant, which is supported by the *ALG3* mRNA levels being compared to the controls. In the  
284 case of *COG5* we postulated that the missense variant could interfere with the formation of lobe  
285 B of the COG complex, causing the unassembled protein to be degraded impairing the  
286 glycosylation pathway in these individuals. This idea was tested by measuring the presence of  
287 *COG6* (another COG protein) in the same samples. *COG6* was present in two distinct molecular  
288 weights (figure 2K and L), with a decrease of the heavier form and an increase in the lighter

289 form. It is possible that this happens due to an increased degradation of COG6 and, being COG6  
290 a COG subunit located in the same lobe but not in direct contact with COG5, this suggests the  
291 destabilization of the whole lobe B by a mutated COG5. This is in accordance with experiments  
292 by Rymen and colleagues showing decreased expression of COG7 (another lobe B subunit) in  
293 COG5-CDG (11).

294 With this data we concluded that the probable cause for both fetal losses was a congenital  
295 defect of glycosylation. We show evidence that the *ALG3* truncating variant results in decreased  
296 protein level, and the *COG5* variant is probably impairing the formation of the COG complex.  
297 Therefore, although both defects individually could lead to a CDG phenotype, we cannot rule out  
298 an effect in the pathway following a “multiple hit” mechanism of disease impacting the N-  
299 glycosylation pathway, starting with the first insult in the ER-related assembly. Although the  
300 presence of the protein is not a guarantee for protein function, it is possible that some residual  
301 *ALG3* activity remains and therefore some glycosylated proteins could be transferred to the  
302 Golgi for further processing. There, the additional COG defect would interfere with Golgi  
303 trafficking, adding a second biochemical abnormality to already decreased glycosylation. We  
304 hypothesize that this could cause truncated glycans similar to a "digenic" mechanism.

305 If this hypothesis is true, we would expect a combined type I/type II glycosylation defect in  
306 our patient, similar to that seen in PGM1-CDG. It is interesting to note that our patient had a  
307 prenatal presentation of skeletal long bone shortening/short stature, congenital heart  
308 malformation and micrognathia, which are also features of PGM1-CDG (14, 15) and have been  
309 observed in some of the COG deficiencies, like COG7-CDG (16).

310 In summary, we have provided evidence indicating a glycosylation defect in this family that  
311 may have impacted fetal development, leading to fetal demise. Interestingly, it is described that



312 protein glycosylation plays a major role in development and maintenance in the third trimester of  
313 gestation – the period when both miscarriages occurred – also supporting this idea (2-4).  
314 Additionally, we show for the first time that studies of glycosylated proteins such as ICAM-1  
315 and LAMP2 can be carried out in cultured amniocytes in the third trimester, leading to the  
316 development of more elaborate and elaborate glycoproteomics techniques in pregnancy losses  
317 suspected with a diagnosis of CDG (17).

## 318 ACKNOWLEDGEMENTS

319 We want to thank the patient’s family for participating in this study and allowing us to  
320 publish these results. We also want to thank Kevin Meyer from the Genomics Laboratory at  
321 Mayo Clinic for his lab work and assisting with amniocyte culturing. This work was funded by  
322 the grant titled Frontiers in Congenital Disorders of Glycosylation (1U54NS115198-01) from the  
323 National Institute of Neurological Diseases and Stroke (NINDS) and the National Center for  
324 Advancing Translational Sciences (NCATS) and the Rare Disorders Consortium Disease  
325 Network (RDCRN) (EM and KR). RTS’s participation in this work was funded by Brazil’s  
326 Programa Institucional de Internacionalização from the Coordenadoria de Aperfeiçoamento de  
327 Pessoal de Nível Superior (PRINT/CAPES). DU’s participation in this work was part-funded by  
328 the Wellcome Trust (ref: 204829) through the Centre for Future Health (CFH) at the University  
329 of York.

330

## 331 REFERENCES

332 1. Ferreira CR, Altassan R, Marques-Da-Silva D, Francisco R, Jaeken J, Morava E.  
333 Recognizable phenotypes in CDG. *J Inherit Metab Dis.* 2018;41(3):541-53.

- 334 2. Altassan R, Peanne R, Jaeken J, Barone R, Bidet M, Borgel D, et al. International clinical  
335 guidelines for the management of phosphomannomutase 2-congenital disorders of glycosylation:  
336 Diagnosis, treatment and follow up. *J Inherit Metab Dis.* 2019;42(1):5-28.
- 337 3. Fisher P, Ungar D. Bridging the Gap between Glycosylation and Vesicle Traffic. *Front*  
338 *Cell Dev Biol.* 2016;4:15.
- 339 4. Ioffe E, Stanley P. Mice lacking N-acetylglucosaminyltransferase I activity die at mid-  
340 gestation, revealing an essential role for complex or hybrid N-linked carbohydrates. *Proc Natl*  
341 *Acad Sci U S A.* 1994;91(2):728-32.
- 342 5. Ungar D, Oka T, Brittle EE, Vasile E, Lupashin VV, Chatterton JE, et al.  
343 Characterization of a mammalian Golgi-localized protein complex, COG, that is required for  
344 normal Golgi morphology and function. *J Cell Biol.* 2002;157(3):405-15.
- 345 6. Karczewski KJ, Francioli LC, Tiao G, Cummings BB, Alföldi J, Wang Q, et al. Variation  
346 across 141,456 human exomes and genomes reveals the spectrum of loss-of-function intolerance  
347 across human protein-coding genes. *bioRxiv.* 2019.
- 348 7. Sparks SE, Krasnewich DM. Congenital Disorders of N-Linked Glycosylation and  
349 Multiple Pathway Overview. In: Adam MP, Ardinger HH, Pagon RA, Wallace SE, Bean LJH,  
350 Stephens K, et al., editors. *GeneReviews((R))*. Seattle (WA)1993.
- 351 8. Lam BL, Zuchner SL, Dallman J, Wen R, Alfonso EC, Vance JM, et al. Mutation K42E  
352 in dehydrodolichol diphosphate synthase (DHDDS) causes recessive retinitis pigmentosa. *Adv*  
353 *Exp Med Biol.* 2014;801:165-70.
- 354 9. Verheijen J, Tahata S, Kozicz T, Witters P, Morava E. Therapeutic approaches in  
355 Congenital Disorders of Glycosylation (CDG) involving N-linked glycosylation: an update.  
356 *Genet Med.* 2020;22(2):268-79.
- 357 10. Paesold-Burda P, Maag C, Troxler H, Foulquier F, Kleinert P, Schnabel S, et al.  
358 Deficiency in COG5 causes a moderate form of congenital disorders of glycosylation. *Hum Mol*  
359 *Genet.* 2009;18(22):4350-6.
- 360 11. Rymen D, Keldermans L, Race V, Regal L, Deconinck N, Dionisi-Vici C, et al. COG5-  
361 CDG: expanding the clinical spectrum. *Orphanet J Rare Dis.* 2012;7:94.
- 362 12. Radenkovic S, Bird MJ, Emmerzaal TL, Wong SY, Felgueira C, Stiers KM, et al. The  
363 Metabolic Map into the Pathomechanism and Treatment of PGM1-CDG. *Am J Hum Genet.*  
364 2019;104(5):835-46.
- 365 13. He P, Srikrishna G, Freeze HH. N-glycosylation deficiency reduces ICAM-1 induction  
366 and impairs inflammatory response. *Glycobiology.* 2014;24(4):392-8.
- 367 14. Altassan R, Radenkovic S, Edmondson AC, Barone R, Brasil S, Cechova A, et al.  
368 International consensus guidelines for phosphoglucomutase 1 deficiency (PGM1-CDG):  
369 Diagnosis, follow-up, and management. *J Inherit Metab Dis.* 2020.
- 370 15. Wong SY, Beamer LJ, Gadowski T, Honzik T, Mohamed M, Wortmann SB, et al.  
371 Defining the Phenotype and Assessing Severity in Phosphoglucomutase-1 Deficiency. *J Pediatr.*  
372 2016;175:130-6 e8.
- 373 16. Medrano C, Vega A, Navarrete R, Ecay MJ, Calvo R, Pascual SI, et al. Clinical and  
374 molecular diagnosis of non-phosphomannomutase 2 N-linked congenital disorders of  
375 glycosylation in Spain. *Clin Genet.* 2019;95(5):615-26.
- 376 17. Abu Bakar N, Lefeber DJ, van Scherpenzeel M. Clinical glycomics for the diagnosis of  
377 congenital disorders of glycosylation. *J Inherit Metab Dis.* 2018;41(3):499-513.